

APPLICATION OF MODEL BASED CONTROL TO ROBOTIC MANIPULATORS

Lyman J. Petrosky, Senior Engineer
 Robotics and Mechanical Design
 Westinghouse Advanced Energy Systems
 Madison, PA 15663

Irving J. Oppenheim, Assoc. Prof.
 Department of Civil Engineering
 Carnegie-Mellon University
 Pittsburgh, Pennsylvania, 15213

ABSTRACT

A robot that can duplicate human motion capabilities in such activities as balancing, reaching, lifting, and moving has been built and tested at Carnegie-Mellon University. These capabilities are achieved through the use of real time Model-Based Control (MBC) techniques which have recently been demonstrated. MBC accounts for all manipulator inertial forces and provides stable manipulator motion control even at high speeds. To effectively demonstrate the unique capabilities of MBC, an experimental robotic manipulator was constructed which stands upright, balancing on a two wheel base. The mathematical modeling of dynamics inherent in MBC permit the control system to perform functions that are impossible with conventional non-model based methods. These capabilities include:

- Stable control at all speeds of operation;
- Operations requiring dynamic stability such as balancing;
- Detection and monitoring of applied forces without the use of load sensors;
- Manipulator "safing" via detection of abnormal loads.

The full potential of MBC has yet to be realized. The experiments performed for this research are only an indication of the potential applications. MBC has no inherent stability limitations and its range of applicability is limited only by the attainable sampling rate, modeling accuracy, and sensor resolution. Manipulators could be designed to operate at the highest speed mechanically attainable without being limited by control inadequacies. Manipulators capable of operating many times faster than current machines would certainly increase productivity for many tasks.

INTRODUCTION

The design of a control system for manipulators is a formidable task due to the complexity of the nonlinear coupled dynamics. The goal is the calculation of actuator torques which will cause the manipulator to follow any desired trajectory. Research has produced many manipulator control schemes ranging from simple Proportional + Integral + Derivative (PID) control to nonlinear feedback control. In a broad sense, two basic categories of control design are found in the literature. The first contains the robust control methods in which the control is able to overpower the system's nonlinear coupled dynamics. The second contains the *model-based* control (MBC) methods in which many of the system nonlinearities are calculated via a system model and the nonlinear system forces are canceled by the actuation forces. For this research we have chosen to use the *Computed-torque model-based* control described in the next section.

Recent advances in computational hardware have made it possible to evaluate in real time the equations of motion of robotic manipulators. Khosla¹ at Carnegie Mellon University (CMU) was the first to demonstrate the feasibility of real time MBC using an inexpensive computer system for control of a six degree of freedom manipulator, the CMU Direct Drive Arm II. The current work builds on this accomplishment and explores additional manipulator capabilities that the existence of real time MBC creates.

PRECEDING PAGE BLANK NOT FILMED

The assumptions required to apply the methods presented here are:

- System is amenable to mathematical modeling
- Suitable control law can be formulated
- Mathematical model and control law can be evaluated in real time
- Necessary physical variables can be instrumented

CONTROL APPROACH

Computed-Torque Control

*Computed-torque*² control is a *model-based* control scheme which strives to use the complete dynamic model of a manipulator to achieve dynamic decoupling of all the joints using nonlinear feedback. The dynamic model of the manipulator is described by the Lagrangian derived equations of motion:

$$\sum_{j=1}^N D_{ij} \ddot{q}_j + \sum_{j=1}^N \sum_{k=1}^N C_{jk}(i) \dot{q}_j \dot{q}_k + g_i = \tau_i \quad \text{for } i = 1, \dots, N. \quad (1)$$

where the q are the joint coordinates. The τ_i are the externally applied joint actuation torques/forces. The inertial D_{ij} , centrifugal and Coriolis $C_{jk}(i)$, and gravitational g_i coefficients of the closed-form dynamic robot model in Equation 1 are functions of the instantaneous joint positions q_i and the constant kinematic, dynamic and gravity manipulator parameters. The kinetic energy gives rise to the inertial and centrifugal and Coriolis torques/forces, while the potential energy leads to the gravitational torques/forces. Actuator dynamics can be incorporated in the dynamic robot model by additions to the Lagrangian energy function.

The *Computed-torque* algorithm begins with a calculation of the required torque to be applied to each of the joints (in vector notation):

$$\begin{aligned} \tau &= \tilde{D}u + \tilde{H} + \tilde{g} \\ \tilde{H}_i &= \dot{q}^T \tilde{C}(i) \dot{q} \end{aligned} \quad (2)$$

where u is the commanded joint accelerations. The "~" indicates that these matrices are calculated from the estimated system parameters. The resulting dynamic equations for the closed-loop system are:

$$\ddot{q} = u - D^{-1} \{ [D - \tilde{D}]u + [H - \tilde{H}] + [g - \tilde{g}] \} \quad (3)$$

If the system dynamic parameters are known exactly, then $\tilde{D} = D$, $\tilde{H} = H$, and $\tilde{g} = g$, then the closed loop system is described by:

$$\ddot{q} = u \quad (4)$$

which is the equation for a set of decoupled second order integrators. The commanded acceleration u_i is then formulated to incorporate the error feedback signal and the reference signal. After decoupling, each joint acts as a second order integrator, therefore the control law is given the form:

$$u_i = \ddot{q}_{id} - 2\zeta\omega(\dot{q}_i - \dot{q}_{id}) - \omega^2(q_i - q_{id}) \quad (5)$$

which causes each joint to act as a second order damped oscillator with natural frequency ω and damping ratio ζ . The form of the equation causes the joint to track the desired joint values q_{id} , \dot{q}_{id} , and \ddot{q}_{id} .

The computed-torque control defined above is based on the assumptions that the system model is accurate and that all joints are actuated. For this research the dynamic parameters of the experimental manipulator were manually measured to provide an accurate system model. We assume in all simulations that the dynamic model is accurate. The second assumption, that all the joints are actuated, does not apply for the experimental system which requires dynamic balancing. However, a suitable control law exists based on the work of Petrosky³. The method, called *hierarchical partitioning*, is directly applicable to the balancing problem, is robust, and gives an intuitive feel for the system's behavior. For the experimental balancing manipulator, the control law, which treats the manipulator as a single inverted pendulum, is merged with the computed-torque control to complete the algorithm.

Determination of Applied Forces

Indirect determination of applied forces (*i.e.* without the use of load sensors) is accomplished by comparison of the manipulator mathematical model and the observed manipulator behavior. A simple example of this is the algorithm for payload determination for the balancing manipulator. Payload estimation can be performed for a balancing manipulator without accurate knowledge of the actuation forces and accelerations, and the required calculation can be performed on-line in real time. Consider the equation of motion for pivoting about the base of the dynamically balanced manipulator:

$$\tau_i = \sum_{j=1}^N D_{ij} \ddot{q}_j + \sum_{j=1}^N \sum_{k=1}^N C_{jk}(i) \dot{q}_j \dot{q}_k + g_i \quad \text{for } i = \text{base joint} \quad (6)$$

The base joint of a balanced manipulator is not actuated, therefore $\tau_i = 0$. However, if the payload value is incorrect, then this equation will evaluate to a non-zero value of τ_i when the observed values of the joint variables are entered. The difference indicates the value of the payload which is given by:

$$\Delta P = - \left(\frac{\partial \tau_i}{\partial P} \right)^{-1} \tau_i \quad (7)$$

where ΔP is the difference between the actual payload and the current estimated value. Under ideal conditions this equation would yield the correct payload value in a single sample; however, the accuracy of the values for \ddot{q}_j can be exceedingly poor if they obtained by double differentiation of position measurements. This was the case in the experimental system, but the problem was overcome by the use of a parameter estimator.

EXPERIMENTAL SYSTEM

Manipulator and Sensors

The experimental manipulator is supported solely on two wheels. It is a double inverted pendulum operating in a plane, and constantly requires active balance motions to prevent falling. The manipulator consists of the servo driven wheeled base, a lower arm section, an elbow joint with drive servo, an upper arm, and an electro-magnet gripper at its tip. It is constructed primarily of aluminum and has a total weight of 13 kg. The two wheels mounted on a single shaft provide effective out-of-plane stability. The tip of the manipulator can reach to a height of 1.8 meters when fully extended, and can be lowered to touch the floor.

The manipulator wheels and elbow joint are each driven by Aerotek servos rated at 1.3 N-m peak torque. The elbow joint has a chain reduction ratio of 57.6:1 and the drive wheels have a chain reduction of 4.8:1. The chain reduced servo arrangement was chosen over direct drive to save weight, and over gear-reduced or harmonic drive to mitigate costly damage in the event of a severe floor collision.

The sensors utilized for manipulator control are:

- Inclination RVDT - a rotary differential transformer measures the angle between the floor surface (via a feeler) and the lower arm.
- Motor Encoders - each servo has an optical encoder of 500 counts per revolution which runs a hardware counter read by the parallel interface board.

Computer Control System

The computer control system hardware consists of a Motorola M68000 based single board computer as the master CPU, a Marince Array Processor Board (APB), an Analog to Digital Converter (ADC) 32 channel input board, a Digital to Analog (DAC) 4 channel output board, a 96 line Parallel Input/Output (PIO) Interface board, and a CRT terminal. The master CPU drives the bus communications, terminal interface, and an interface to a VAX computer. The VAX computer serves as the disk storage for the system programs and as the post processor of the experimental data.

The Marince array processor is a high speed programmable single board processor with an instruction cycle of 125 ns. It is used to perform the calculation intensive operations required to implement MBC. The board has fixed point multiplier and addition hardware which are used for floating point operations. The floating point addition or multiplication routines execute in approximately 1 μ s. Negation requires 125 ns. Computation of the sine/cosine pair requires 15 μ s. Additional routines perform data type conversion and other functions required to format the sensor data.

Processing for *real time control* is done by the Marince processor exclusively. Manipulator trajectory calculations are handled by the M68000 CPU on a time sharing basis. In operation a timer interrupts the CPU at each sampling instant. The CPU copies the sensor data to the Marince array processor memory, and initiates Marince execution. The Marince formats the data, does scaling operations, performs the trigonometric functions, and then calculates the inverse dynamics. The formatted output data is ready in less than 0.5 ms. The Marince returns to control data to the CPU which outputs it to the DAC's. The cycle time is fast enough that the control algorithm and dynamic model can be evaluated at a sampling frequency in excess of 1000 Hz.

EXPERIMENTAL RESULTS

The experimental manipulator was fully reliable in maintaining balance for long periods while performing a variety of tasks. The base moves approximately ± 3 mm to maintain balance and the tilt varies by ± 0.0063 rad. This motion does not indicate a flaw in the balancing algorithm, but rather the motion results from being at the limit of tilt resolution of the RVDT sensor used with the floor feeler; the RVDT signal variation corresponds to the magnitude of a single digital count. Because the base dimension of the experimental system is zero, it is physically impossible for the manipulator to balance without some on going motion.

The manipulator proved very resistant to upset; its recovery ability appears to exceed that of a human under similar magnitude disturbances. Figure 1 records the transient response of the manipulator to a severe impact (base position q_1 and tilt q_2). The manipulator moved forward to balance and then quickly returned to the original position. The manipulator was also forgiving (compliant) of collision. The manipulator would bounce lightly off an obstacle and come to rest simply leaning against it. When commanded to back away from the obstacle, the manipulator would resume balancing as soon as contact was broken.

Figure 2 records the transient response of the manipulator under two cycles of application of a payload of 0.811 kg, suddenly added or removed. The payload compensation algorithm quickly determines the new payload and adapts the control, restoring the manipulator to its original position. It was possible to carry large payloads with the experimental manipulator. The manipulator used its own weight to balance and transport payloads ranging up to 3.2 kg, which is 25% of its system weight, without difficulty. The results of payload estimation in a non-transient condition show a noise level of only ± 26 gm which is 0.2% of the system mass.

Another payload experiment successfully demonstrated the development and control of lateral force through the motion of system masses. A rope attached the manipulator to a heavy mass on a horizontal surface, and the manipulator was used to pull the mass across the table, against the force of friction, for some target distance. The manipulator developed a lateral force through the movement of its center of mass to a point behind its wheel axis, producing a resulting force in the rope; the system displays balance through the movement which ensues when the lateral force reaches and exceeds the friction force. The manipulator thereby demonstrates the approach used by a human to pull a heavy weight across a floor.

CONCLUSIONS

The feasibility of utilizing real time Model Based Control (MBC) for robotic manipulators has been demonstrated. The experimental results demonstrate the effectiveness of the control approach and of the payload estimation/adaptation algorithm developed for this effort. The mathematical modeling of dynamics inherent in MBC permit the control system to perform functions that are impossible with conventional non-model based methods. These capabilities include:

- Stable control at all speeds of operation;
- Operations requiring dynamic stability such as balancing;
- Detection and monitoring of applied forces without the use of load sensors;
- Manipulator "safing" via detection of abnormal loads.

This work demonstrates an initial implementation of the above features for a robotic manipulator.

The full potential of MBC has yet to be realized and much work remains to be done. The experiments performed for this research are only an indication of the potential applications. Unlike conventional PID control, MBC is a theoretically complete control algorithm with no inherent stability limitations. Its range of applicability is limited only by the attainable sampling rate, modeling accuracy, and sensor resolution. Manipulators could be designed to operate at the highest speed mechanically attainable without being limited by control inadequacies. Manipulators capable of operating many times faster than current machines would certainly increase productivity for many tasks. These manipulators could also have build in safing in response to abnormal loading conditions.

ACKNOWLEDGMENTS

The research¹ was performed for the Department of Energy, Advanced Reactor and Nuclear System Technology Support, Program NE-85-001. We are indebted to the Department of Energy for sponsorship of this research under contract DE-AC02-85NE37947, *Dynamic Stability for Robot Vertical Reach and Payload*, and to Clint Bastin of DOE for his particular interest and support. We are also most grateful to Westinghouse AES for their cooperation in accommodating the residence of Mr. Petrosky at Carnegie-Mellon. Finally, we wish to acknowledge the contributions of Professor I. Shimoyama, Professor J. Bielak, and graduate student Eric Hoffman.

REFERENCES

1. Khosla, P.K., *Real-Time Control and Identification of Direct-Drive Manipulators*, PhD dissertation, Carnegie-Mellon University, 1986.
2. Markiewicz, B.R., "Analysis of the Computed-Torque Drive Method and Comparison with the Conventional Position Servo for a Computer-Controlled Manipulator", Technical Memorandum 33-601, Jet Propulsion Laboratory, Pasadena, CA, March 1973.
3. Petrosky, L.J., "Problem Structuring Applied to the Design of a Controller for the Stabilization of a Double Inverted Pendulum", Master's thesis, Carnegie-Mellon University, 1986.

¹Disclaimer: The view, opinions, and/or findings contained in this report are those of the authors and should not be construed as an official U. S. Department of Energy or Carnegie-Mellon University position, policy or decision, unless designated by other documentation.

PATENT STATUS: This document copy, since it is transmitted in advance of patent clearance, is made available in confidence solely for use in performance of work under contracts with the United States Department of Energy. This document is not to be published nor its contents otherwise disseminated or used for purposes other than that specified, before patent approval for such release or use has been secured upon request from the Patent Counsel, U.S. Department of Energy.

ORIGINAL PAGE IS
OF POOR QUALITY

7

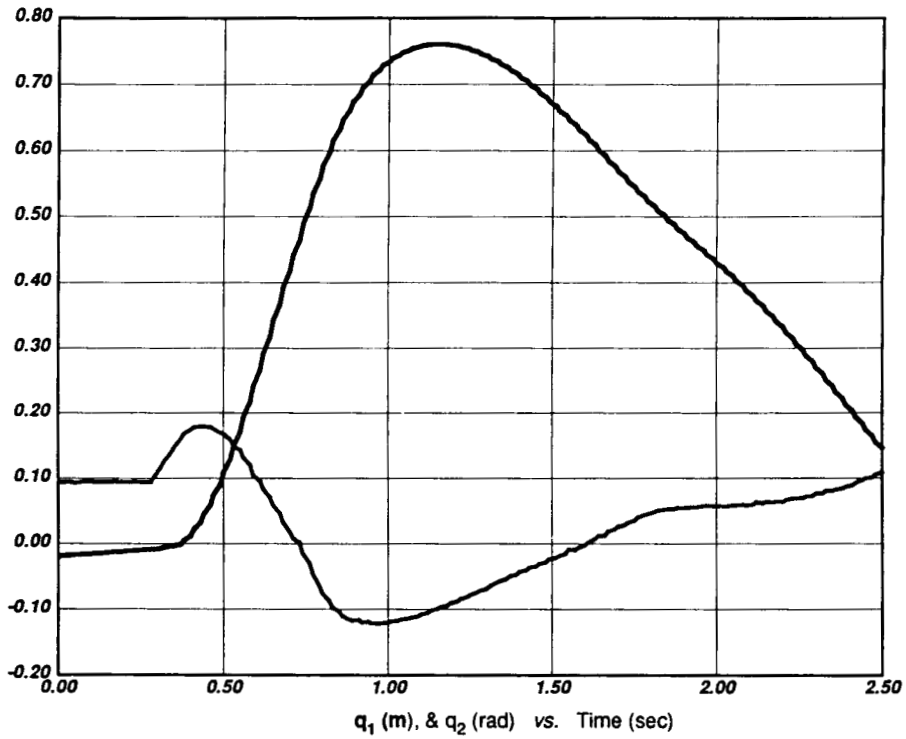


Figure 1: Response to a Lateral Impulse Load at 0.3 Seconds

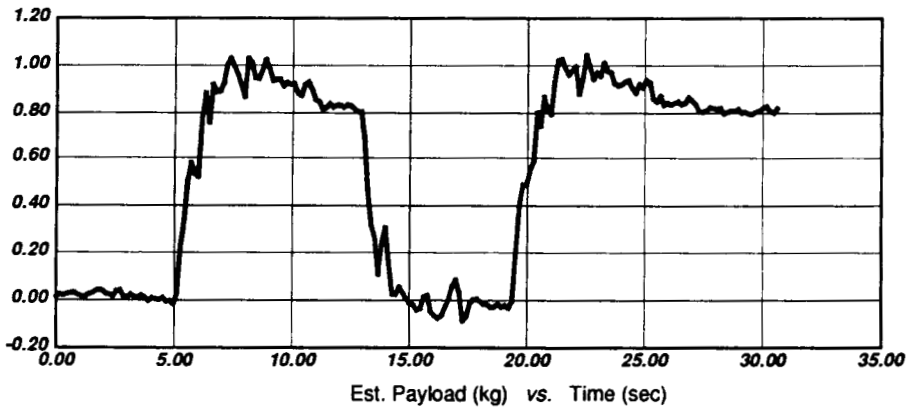


Figure 2: Payload of 0.81 kg Applied On/Off/On